Colloids and Surfaces A: Physicochemical and Engineering Aspects 676 (2023) 132199

Contents lists available at ScienceDirect

Colloids and Surfaces A: Physicochemical and Engineering Aspects

journal homepage: www.elsevier.com/locate/colsurfa

How char from waste pyrolysis can improve bitumen characteristics and induce anti-aging effects

Valentina Gargiulo [a], Michela Alfe [a,*], Giovanna Ruoppolo [a], Francesco Cammarota [a], Cesare Oliviero Rossi [b], Valeria Loise [b], Michele Porto [b], Pietro Calandra [c,*], Mikolaj Pochylski [d], Jacek Gapinski [d], Paolino Caputo [b]

[a] National Research Council, Institute of Sciences and Technologies for Sustainable Energy and Mobility, CNR-STEMS, P.le V. Tecchio 80, Napoli 80125, Italy
[b] University of Calabria – Department of Chemistry and Chemical Technologies, Via P. Bucci Cubo 14D, Rende, CS, 87036, Italy
[c] National Research Council, CNR-ISMN, Strada provinciale 35 D n.9 - 00010 Montelibretti (RM) - Italy, Monterotondo Stazione, RM 00015, Italy
[d] Faculty of Physics, Adam Mickiewicz University, Uniwersytetu Poznanskiego 2, Poznan 61-614, Poland

HIGHLIGHTS

- Re-using solid residues from the pyrolysis of wastes can improve bitumens characteristics.
- The char coming from the pyrolysis of waste tyres can act as anti-aging additive in bitumen.
- Anti-aging effect in bitumen is due to its carbonaceous nature and its better char dispersion in bitumen.

GRAPHICAL ABSTRACT

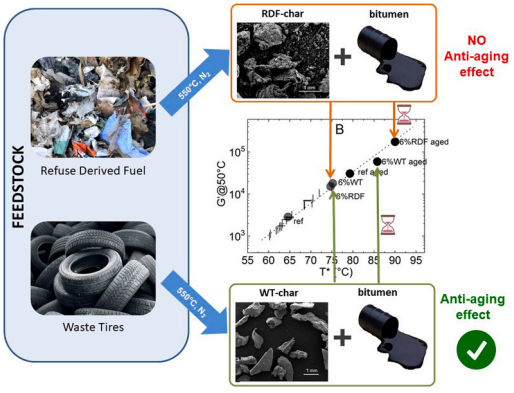

ARTICLE INFO

Keywords:
Waste pyrolysis
Char
Anti-aging effect
Activated carbon bitumen
Rheology

ABSTRACT

Modifying bitumens to improve their characteristics is one of the ways to increase road pavement durability reducing maintenance costs and environmental issues. In this study the structural and mechanical characteristics of a 50/70 bitumen modified by two different char samples are presented. The choice of char as bitumen modifier fulfils the recent needs for environmental protection. The two char samples come from the pyrolysis of Refuse Derived Fuel (RDF) and waste tyres (WT), respectively. They differ in composition and morphology and their production took place with different yields. Char-modified bitumens revealed increased shear modulus and resistance to mechanical stress as found by rheometry. Artificial aging of these char-modified bitumens unveiled that the bitumen modified by char from WT (WT-char) possessed a certain resilience against aging, with a reduced increase in rigidity upon aging. The anti-aging effect showed by WT-char was attributed to its higher

* Corresponding authors.
E-mail addresses: michela.alfe@stems.cnr.it (M. Alfe), pietro.calandra@cnr.it (P. Calandra).

https://doi.org/10.1016/j.colsurfa.2023.132199
Received 16 June 2023; Received in revised form 31 July 2023; Accepted 4 August 2023
Available online 6 August 2023

carbon content, which confers higher compatibility with the bitumen chemical nature and presumably a more uniform dispersion within the bituminous structure thanks to the establishment of more effective interactions.

1. Introduction

In recent years, greater attention towards conscious use of natural resources is being paid, with efforts to minimize input of resources and output of wastes [1]. Legislation itself fosters a transition to a regenerative circular economy [2]. Research cannot be, of course, insensitive to this change, with a definite guide towards a reuse of raw materials and a reduction of waste products [3]. In this ambit, designing highly performing asphalts would allow for an extension of the road pavements lifetime with consequent environmental and economic benefits [4,5]. Not only a more durable road pavement reduces maintenance costs but also its substitution, once exhaust, with a new one is pushed to the future, with an ultimate reduction of wastes and use of new materials. If the production of a more performing asphalt is obtained, in turn, by re-utilization of wastes coming from other human activities, than an ideal matching would be achieved, with a virtuous coupling of the two processes [6]. Various methods to improve asphalts have been setup. They generally consist in adding specific materials to bitumen, which is the organic-based binder of the asphalts, and which has a pivotal role in the overall performances. For example, small particles have been found to exert significant effects on the rheological properties of bitumen thanks to their peculiar characteristics (high surface-to-volume ratio, tunable chemical constitution, etc.) even when added in few percent [7]. In fact, they can increase the capacity of the road pavement load and decrease cracks due to fatigue during the operation life. Of course, different particle sizes give different effects: particles in the range 10^{-5}-10^{-2} m (micro-scale) are used for conventional pavements [8,9] whereas smaller particles are used for high-strength and high-performance asphalts [10,11].

A simple chemical consideration can be now made: carbonaceous particles are expected to give better results thanks to their chemical compatibility with the bitumen chemical nature (they both are organic-based materials) [12]. This allows a link with another activity to reduce civil wastes, namely the pyrolysis of urban wastes. Pyrolysis, in fact, is an oxygen-free thermal degradation process converting materials into:

- combustible gases [13];.
- a liquid rich in hydrocarbons and oxygenated species (i.e. the oil, mainly consisting in a combination of organic molecules used for several applications and that can be obtained also by pyrolysis of vegetable biomass – bio-oil – like food waste or cellulose [14–17]);.
- and, most importantly for our purposes, a solid residue (char) [18,19] with a high carbon content which can be well accommodated in the organic-based bitumen structure.

Optimal ranges of temperature, heating rate, and gas residence time have been defined for the maximization of each type of product.

Pyrolysis process has undisputed advantages in the urban waste treatment [20], and its solid products would become here added value additives in the production of improved bitumens, coupling the two processes in a circular economy vision.

Char falls within the definition of *activated carbon*, i.e. a carbonaceous material heated at high temperatures for long times (hours). The use of activated carbon for several applications like filtration, cleaning, adsorption of gases, liquids and contaminants [21,22] is consequence of the peculiar and interesting physico-chemical properties of such kind of a material, so interesting behavior can be foreseen also in bitumen applications. In addition, in this specific application, char could be an ideal additive also for its porous/fibrous structure allowing in principle strong interactions with the bituminous matrix [23].

The physico-chemical idea inspiring the present work is that the presence of solid particles, homogeneously dispersed within the bitumen, could slow down the kinetical processes (translational, rotational, collective…) of the molecules making part of the bituminous structure by imposing them an effective solid interfacial barrier hindering some of their degrees of freedom. Further chemical effect coming from the activated carbon surface reactivity can also be envisaged, in our opinion.

The goodness of this idea is witnessed by some anti-oxidation effects discovered by Rajib et al. in 2021 [24], and by the increased thermal storage stability found in the same year by Kumar et al. [25] who was studying binders modified with pyrolyzed plastic wastes.

For this reason, in this work two different char samples, produced from different civil wastes, have been analysed as modifiers and as anti-aging additives for bituminous materials. To achieve safe data interpretation, chemico-physical and morphological characterizations of the two char samples as well as the parent wastes were performed, whereas the mechanical characteristics of the bituminous materials were characterised by rheometry as a function of temperature. Data comparison will give a framework of utmost importance for future efficient production of char and its application [26].

2. Experimental

2.1. Materials

The refuse derived fuel (RDF) was supplied by Calabra Maceri srl (Rende, CS, Italy). The RDF feedstock was characterized by a non-homogeneous aspect with pieces large about 3 cm. Its average composition, and the proximate, ultimate and calorimetric analysis results are reported in a previous work [27], and partially in Table 1 for sake of completeness. The high volatiles content (above 80 wt%) and the high carbon content (48 wt%) are ascribable to the high content of plastics and paper-based materials. The ashes (9 wt%) consist primarily of alkali and alkali earth metal-containing minerals (calcium-based compounds are the most abundant species).

The feedstock made of scraped waste tires (WT) presents an overall homogenous aspect and was grinded at about 0.8 mm before use. Its composition is estimated by ultimate and proximate analyses and reported in Table 1. The high volatiles (above 60 wt%) produced during pyrolysis and the high carbon and sulphur contents (~80 wt% and ~2 wt%, respectively) in the feedstock are ascribable to the rubber components. Also in the case of WT, the ash content is not negligible (6.7 wt %). The most abundant metallic species in the ashes was zinc, in accordance with other literature findings [28].

The bitumen used in this study was produced in Saudi Arabia and it was supplied by Lo Prete (Italy). Its penetration grade was found to be 50/70 as measured by the usual standardized procedure [29] in which a standard needle is loaded with a weight of 100 g and the length traveled

Table 1
Feedstock and char composition.

Feedstock	RDF		WT	
Sample	RDF[27]	RDF-char	WT	WT-char
Ultimate analysis				
C (wt%)	48.4	30.9	82.3	88.8
H (wt%)	6.85	0.28	6.10	0.03
N (wt%)	0.39	0.29	0.10	0.10
S (wt%)	0.30	0.56	2.30	3.20
Proximate analysis				
Humidity (wt%)	1.61	4.46	0.49	1.60
Volatiles (wt%)	80.7	24.1	64.6	6.2
Ashes (wt%)	9.05	49.2	6.70	12.5
Fixed carbon (wt%)	8.70	22.2	28.3	79.7

into the bitumen specimen is measured in tenths of a millimeter for a known time, at fixed temperature. Its characteristics were determined in previous works [30,31].

2.2. Method

2.2.1. Pyrolysis tests and characterization

The pyrolysis experiments were conducted in a reactor equipped with a prototype macro-thermobalance (macro-TGA), using the experimental setup shown in the scheme reported as Fig. S1 of the supporting information section. The samples (around 100 g for each run) were placed in a stainless steel cylindrical vessel (d = 0.90 dm, h = 3 dm, V = 2.13 dm^3) equipped with two load cells (model Mettler Toledo single point and capacity ranges up to 3 Kg) and heated up to 550 °C applying a heating rate around 30 °C/min. The pyrolysis test lasted approximately 2 h. A constant flow rate of pure nitrogen (3.9 Ndm^3/h) was used to establish an inert atmosphere inside the chamber. For all tests, the pressure was set to 1 bar. Load cells, heating module, vessel and sample temperature were recorded by means of a National Instrument USB-6251 data acquisition system. Bio-oil was collected by condensing the outlet vapor stream. Char was recovered from the reactor at the end of the experimental test, and the yield was determined gravimetrically with respect to the fed feedstock. The pyrolysis test was performed twice on each feedstock.

Proximate analysis to determine feedstock humidity, volatile, ashes and fixed carbon contents was performed on a LECO 701 thermobalance according to the standard ASTM D7582–15. Each measure was repeated 3 times.

C, H, N, S contents were determined by ultimate analysis in accordance with ASTM D3176–15 and ASTM D4239 standards. C, H, N contents were determined by using a LECO 628 analyser after EDTA calibration (measurements were performed in triplicates). Sulphur content was determined by a LECO CS 144 analyser calibrated with a high content (vanadyl sulphate pentahydrate) and a low content (low sulphur coal Leco 502–681) sulphur reagents (measurements were performed in duplicate).

The content of inorganic species was estimated by inductively coupled plasma-mass spectrometry (ICP-MS) using a Agilent 7500 instrument, after a microwave-assisted acidic treatment of the materials in accordance with US-EPA 3051 and 3052 methods.

The thermal behavior of the feedstocks and of solid pyrolysis products (char) was investigated through thermogravimetric analyses on a Perkin-Elmer STA6000 in inert (N_2, 40 mL/min) or oxidizing (air, 40 mL/min) atmospheres. Each material was heated from 30 °C up to 800 °C applying a heating rate of 10 °C/min. 5–20 mg of material was loaded in an alumina crucible for each measurement. The alumina crucible was previously treated in furnace at 920 °C to guarantee an accurate solid residue determination.

The morphology of both feedstocks and the resulting char samples was evaluated by scanning electron microscopy (SEM) imaging using a FEI Inspect microscope equipped with an EDS Oxford AZtecLiveLite probe and Xplore 30 detector for elemental analysis. The powdered samples were previously dried and sputter-coated with a thin layer of gold to avoid charging.

To analyze the morphology of char, an amount of each char was dispersed in silicone oil (about 0.15% wt/wt) and sonicated in a commercial low-power sonicator for few (4−5) hours and then analyzed by SEM imaging.

The surface chemistry of the char samples was investigated by infrared spectroscopy measuring FT-IR spectra in the 450–4000 cm^{-1} range on a Perkin–Elmer Frontier MIR spectrophotometer operated in transmittance mode. The spectra were acquired on KBr pellets (2 wt%), collecting 8 scans for each measurement and correcting the background noise.

The crystallinity of char samples was investigated by X-ray powder diffraction (XRD) analysis in the 2θ range 3–90° using a Rigaku Miniflex 600 automated diffractometer equipped with CuKα radiation source.

2.2.2. Bitumen preparation and characterization

Addition of char to bitumen was carried out in the following way: char was added to fully flowing hot bitumen (150 ± 10 °C) to achieve the desired final char content of 6% w/w. The mixture was stirred at 500–700 rpm by a mechanical stirrer (IKA RW20, Königswinter, Germany) for 30 min at the same temperature to allow for homogenization of the blend. In our experience such conditions are the best to assure the preparation of homogeneous samples: at lower rpm samples homogenization is not effective, while above 700 rpm the bitumen can be oxidized due to the abrupt increase in bitumen-air interface in the vortex formed during stirring, as well as to obvious increased interfacial kinetics, with possible consequent change in the final bitumen rheological properties. This method is regarded as a standard operative procedure and it has also been reported by other authors [32]. After mixing, the resulting bitumen was poured into a small sealed can and then stored in a dark chamber at 25 °C to retain the desired morphology. Due to the sensitivity of such materials to the annealing time [33], and due to the comparative spirit of our work, we took care that all our samples had the same temperature cooling rate (5 °C/min) and annealing time (15 min).

A standard filler-free bitumen sample was used as reference, hereafter labeled as “ref”.

Aging of the samples was carried out by the RTFOT procedure, (Rolling Thin-Film Oven Test) according to ASTM D2872–04 with the only exception that the aging time was set at 225 min instead of the normally adopted 75 min. The reason for this is to obtain bitumens rigid enough to simulate a prolonged aging process of about 10–12 years, which is a typical asphalt life-cycle.

In Dynamic Shear Rheological (DSR) tests the complex shear modulus [34] $G^* = G' + i\,G''$ was measured in the regime of small amplitude oscillatory shear at 1 Hz as a function of temperature (temperature controlled by a Peltier element, uncertainty ± 0.1 °C) by dynamic stress-controlled rheometer (SR5000, Rheometric Scientific, Piscataway, NJ, USA) equipped with a parallel plate geometry (gap 2 mm, in agreement with literature work [35]; diameter 25 mm) in the regime of small-amplitude oscillatory shear [36]. The real and imaginary parts define the in-phase (storage, measure of the reversible elastic energy) and the out-of-phase (loss, irreversible viscous dissipation of the mechanical energy) moduli, respectively [37]. The experimental conditions were chosen after preliminary stress-sweep tests to guarantee linear viscoelastic conditions in all measurements. Temperature ramp tests (time cure) were carried out aiming at investigating the material phase transition, so temperature was progressively increased from 25 °C to 95 °C at 1 °C/min and applying the proper stress values to guarantee linear viscoelastic conditions at all tested temperatures.

3. Results and discussion

3.1. Char chemical characterization

The pyrolysis of WT led to a char yield (64.9 wt%) higher than that of RDF (42.3 wt%); such a difference is ascribable to the different chemical composition of the two feedstocks (see Table 1). More in detail, WT is an overall homogeneous feedstock mostly composed of carbon (82.3 wt%, Table 1) and during the thermal decomposition it generates an amount of volatiles up to 64.6 wt% leaving a solid residue made by ashes (~7 wt %) and fixed carbon (~28 wt%), as reported in the last rows of Table 1. In contrast, RDF is a highly heterogeneous feedstock, as already shown in ref [27], composed of only 48 wt% of carbon. During the thermal decomposition it generates a high amount of volatiles (up to ~80 wt%) leaving a solid residue made by ashes (~9 wt%) and fixed carbon ~ 9 wt %. For the sake of completeness, the results of thermogravimetric analyses of both feedstocks, under both inert and oxidative atmospheres are reported as Figs. S2 and S3 in the supporting materials section.

The two char samples differ in terms of physical structure, chemical

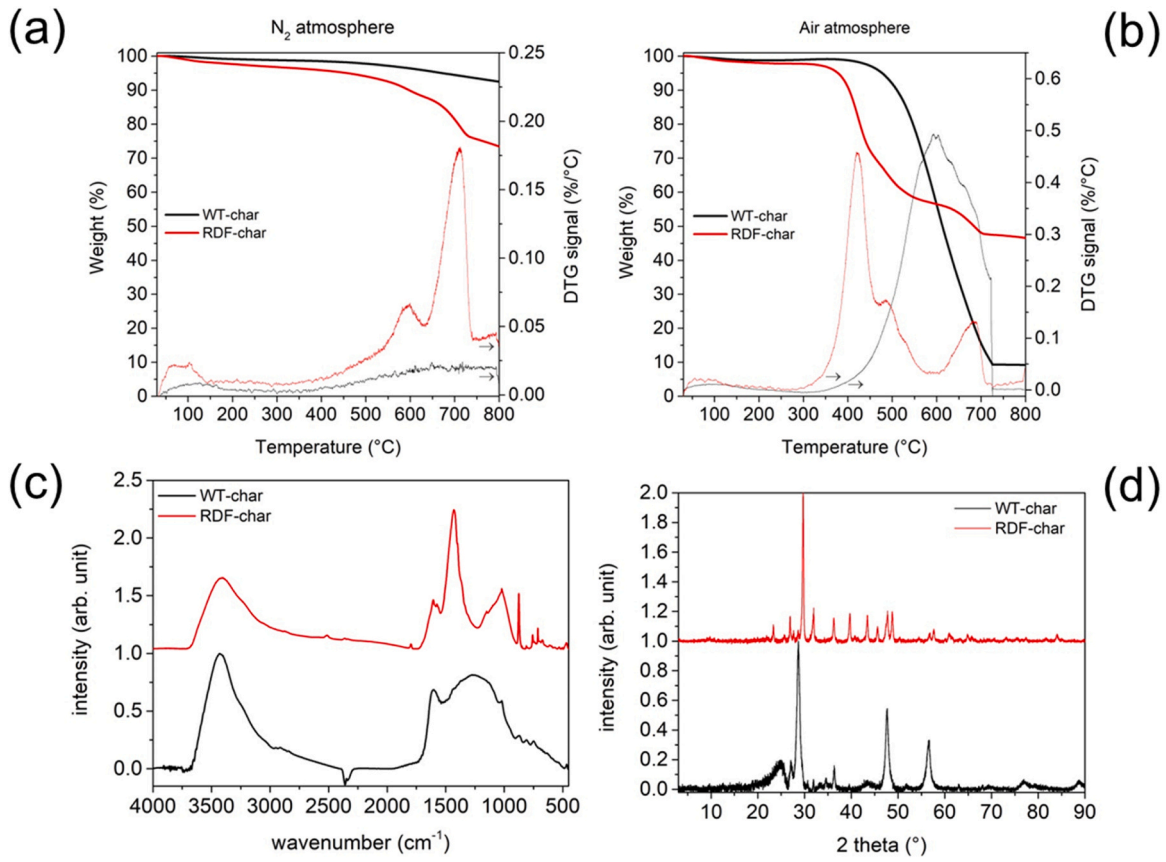

Fig. 1. Upper panels: Thermogravimetric plots of RDF-char (black) and WT-char (red) at 30 °C/min, in N_2 (a) and air atmosphere (b) and the corresponding derivative (DTG) curves; Lower panels (c): height-normalized FTIR spectra of RDF-char (black) and WT-char (red); (d): height-normalized XRD patterns of RDF-char (black) and WT-char (red).

composition, thermal behavior and surface chemistry (see Table 1 and Fig. 1) as described in the following.

The char obtained by WT pyrolysis (hereinafter WT-char) shows a quite high carbon content (88.8 wt%), a very low hydrogen content (0.03 wt%) and a not negligible ulphur content (3.2 wt%). These compositional values are in line with other literature findings [38]. WT-char is also characterized by a high thermal stability both in an inert (N_2) and an oxidizing (air) atmosphere, as testified by the results of the thermogravimetric analyses reported in Fig. 1 (panels a and b). The profile of WT-char TG analysis under nitrogen atmosphere, indeed, highlights a very slow weight decrease leading to a solid residue around 92.5 wt%, that corresponds roughly to the sum of fixed carbon and ashes evaluated by proximate analysis (see Table 1). The profile of WT-char TG analysis under oxidative atmosphere, at converse, is characterized by a main thermal event peaked around 600 °C ascribable to the burn-off of the material. A temperature of burn-off above 550 °C is typical of materials with a good degree of graphitization like activated carbons, bio-char, combustion derived products as seen in refs [39,40]. The presence of a good degree of graphitization in the WT-char structure is also demonstrated by the shape exhibited by the FTIR spectrum reported in Fig. 1 panel c, resembling that of a graphitic amorphous carbon [39,40]. In particular, the FTIR spectrum of WT-char is characterized by a broad band in the 3000–3700 cm^{-1} range related to O-H stretching vibrations (also due to possible adsorbed H_2O), overlapping bands at 1100–1600 cm^{-1} due to the skeletal vibration of C-C, C═C and C═O bonds of the carbonaceous network and low intense bands between 700 and 1000 cm^{-1} ascribable to the bending of aromatic out of plane C-H bonds [39]. The WT-char can be considered a mixture of amorphous and crystalline material on the basis of its XRD pattern (Fig. 1, panel d), in which a broad band peaked around 25 2θ° ascribable to amorphous carbon and broad peaks between 25 and 60 2θ°, ascribable mainly to ZnS and ZnO, can be detected [41]. ZnO is a typical additive used to facilitate rubber vulcanization. Its presence is evident already in the WT prior to pyrolysis (see Fig. S4 in Supporting Information). During the waste tire pyrolysis process, ZnO retains sulfur forming ZnS as a consequence of the reaction with H_2S evolving from the decomposition of the rubber sulfur compounds resulting from the vulcanization process. The presence of ZnS in pyrolytic char derived from waste tires has been reported by different authors [41–44]. In this framework, of reference is the work of Darmstadt et al. [43], which first demonstrated that, with increasing pyrolysis temperature, zinc oxide converts into zinc sulfide (ZnS).

Debye-Sherrer analysis of the XRD peak allows an estimation, through determination of the Full Width at Half Maximum, of the order parameter. Its meaning is the distance at which the order is lost, basically as a consequence of the finite size of scattering domain. Wider widths imply loosening of the order at shorter distances giving smaller order parameter values. The typical size of the carbonaceous particles scattering domains is rather low, of about 3–4 nm, confirming the mostly amorphous nature of such particles. As for the ZnS particles, their scattering domain size is assessed to be of about 10 nm.

The presence of zinc-based compounds on the WT-char surface was probed by EDX analysis (Fig. 2, (a-b) and supporting info, Fig. S5). This element (together with S, Si, Co) resulted to be homogeneously dispersed in the sample, as evidenced by EDX elemental mapping reported in Fig. 2 on two different specimen sectors and furthermore by the individual element maps reported in the supporting info (Fig. S5).

The char obtained by RDF pyrolysis (hereinafter RDF-char) is characterized by a lower carbon content (30.89 wt%) with respect WT-char and also by a lower thermal stability. The profile of RDF-char TG

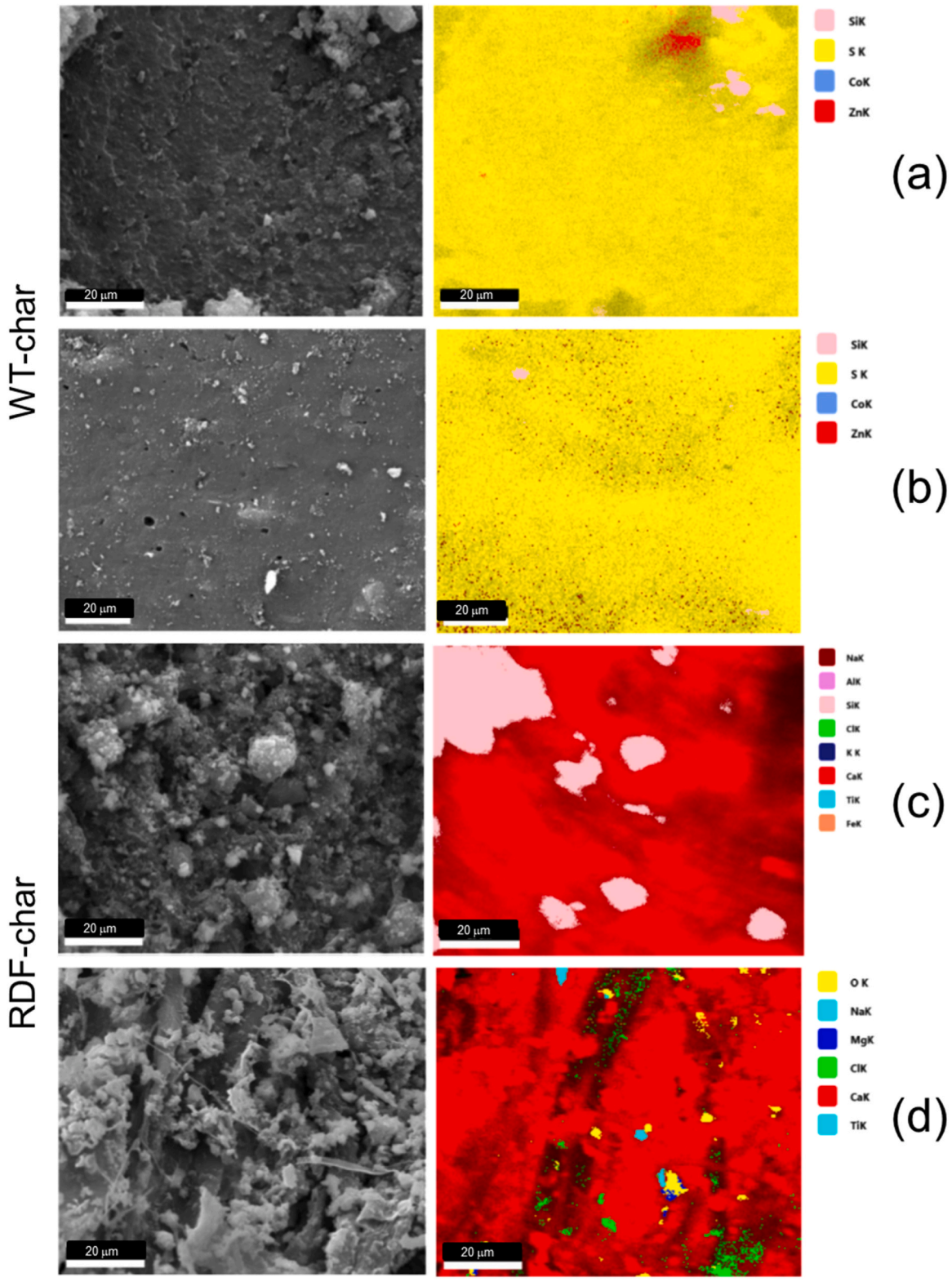

Fig. 2. EDX elemental mapping (element overlay maps) of WT-char (a-b) and RDF-char (c-d).

analysis under nitrogen atmosphere (Fig. 1, panel a) is characterized by two thermal events, one peaked around 580 °C and another around 700 °C probably due to the decomposition of inorganic components present in the ashes [27]. The amount of the solid residue is ~73.5 wt% and it corresponds roughly to the sum of the expected ashes and fixed carbon, as established by proximate analysis (see Table 1). Differently, the profile of RDF-char TG analysis under oxidative atmosphere (Fig. 1, panel b) exhibits three main different weight losses: one peaked at 410 °C, one peaked around 500 °C and one peaked around 680 °C. The presence of thermal events at a temperature below 500 °C are indicative of a propensity of the material to decompose, namely of a less stable structure; anyway, the occurrence of thermal events at a temperature below 500 °C can be the result of catalytic phenomena induced by the high ash content (above 45 wt%). This thermal behavior is in line with

that reported by Haykiri-Acma et al.[45], who studied the influences of Devolatilization Severity on char from a RDF. The different structure of RDF-char with respect that of WT-char has been highlighted also by infrared spectroscopy measurements. The FTIR spectrum of RDF-char reported in Fig. 1, panel c, indeed, is characterized by a broad band in the region between 3000 and 3700 cm^{-1} due to O-H stretching vibrations (also due to possible adsorbed H_2O), a band peaked around 1580 cm^{-1} ascribable to the skeletal vibration of C═C and/or C═O bonds (of lower intensity than in the case of WT-char due to the lower carbonaceous nature), an intense band peaked around 1480 cm^{-1} and less intense bands below 1250 cm^{-1} ascribable to vibrational modes of inorganic components [46].

The crystallinity of RDF-char was probed by XRD and the resulting pattern is reported in Fig. 1d. Looking at the XRD pattern of RDF-char (see Fig. 1d), it is worth of note that the diffraction peaks ascribable to the inorganic components (mainly $CaCO_3$ -calcite- [45,46]) as inferred by elemental analysis (Fig. 2 and Fig. S6 in the supporting info) prevail on the broad peak expected for the amorphous carbon fraction. Debye-Sherrer analysis of the XRD pattern shows that the order parameter is higher than that found in WT-char, being of the order of several tens nanometers. Although it is not representative of the overall particle size, the higher value in RDF-char than in WT-char indicates a certain tendency of the former to produce bigger domains, an aspect which will be reflected to the overall final particle (see particle size analysis below). The presence of $CaCO_3$ as inorganic component of RDF-char can be explained considering that Calcite is used as binder in the wastepaper or as filler in low grade plastics [46], namely two of the most abundant components of the RDF used as feedstock for the pyrolysis process in this work (5.4% and 84%, respectively [27]). By EDX elemental mapping reported in Fig. 2(c-d) on two different sample sectors, an inhomogeneous feature can be found. This aspect is further evidenced by the individual element maps reported in the supporting info (Fig. S6).

3.2. Char morphological characterization

The morphology of the two char samples has been investigated by SEM imaging (Fig. 3): for WT-Char, a compact aspect with quite a regular surface has been highlighted whereas, for RDF-char, a fiber-like structure is present, probably deriving from the cellulose-containing components of the starting feedstock, in agreement with previous findings [27,45]. In addition, the morphology of RDF-char is that typical of an inhomogeneous material, confirming the clues from EDX elemental analysis. Further images, recorded at higher magnifications, are available in Supporting Information (Fig. S7).

As it can be seen from SEM images, both char samples show millimeter and sub-millimeter particles, with RDF-particles seeming slightly bigger than WT ones. However, these particles are bare aggregates of smaller particles loosely stuck together, which easily disassemble during their manipulation and, in particular, during their mixing with hot bitumen and successive stirring to form the char-bitumen composite. The final char-containing bitumen, in fact, does not possess such big mm-scaled (or sub-mm) particles, being quite homogeneous even at the micrometer scale. To find out the size distribution of the individual particles, the char samples were dispersed in silicone oil and sonicated in a commercial low-power sonicator. This treatment should somehow stimulate char dispersion as it really takes place during the preparation of char-containing bitumens. From the chemical point of view, in fact, silicone oil quite well reproduces the basic apolar character of the bitumen, a similarity inspiring previous research in this sense [47]; on the other side, from the dynamic point of view, silicone oil viscosity reproduces the viscosity of the bitumen at the high temperature (150 °C) used during its mixing with char. Finally, sonication should somehow speed up char dispersion, having a similar effect with respect to the prolonged stirring. It is obvious that this treatment helps in disaggregating the big char assemblies and must be considered just a model of the bitumen preparation procedure. The microscopy investigation we are presenting therefore has the role of helping in unveiling the size distribution of the "individual" particles making the char in the bitumen. Of course, the detailed investigation of the effective char state *within* the bitumen will need different and ad-hoc techniques, since the bituminous matrix is quite dark and opaque at the visible light, making optical microscopy hard to perform, and being the SEM investigation basically a surface investigation which can probe the inner layers only with specific strategies, all this going beyond the scope of this manuscript. The size distribution for both char samples after aggregates disassembling in silicone oil is reported in Fig. 3 right panel. It must be first noted that the sizes of the particles for both char samples fall mostly below the value of 1 μm and do not match the sizes of scattering domains derived by XRD (nm-sized). The difference of at least one order of magnitude indicates that the char individual particles can be made of different domains and/or being polycrystalline. The difference between the sizes observed in XRD and SEM can be therefore ascribed to this.

In addition, it can be noted that WT-char is more abundant in particles with size below 0.5 μm than RDF-char. On the contrary, RDF-char contains more particles with size above 0.5 μm than WT-char. The size

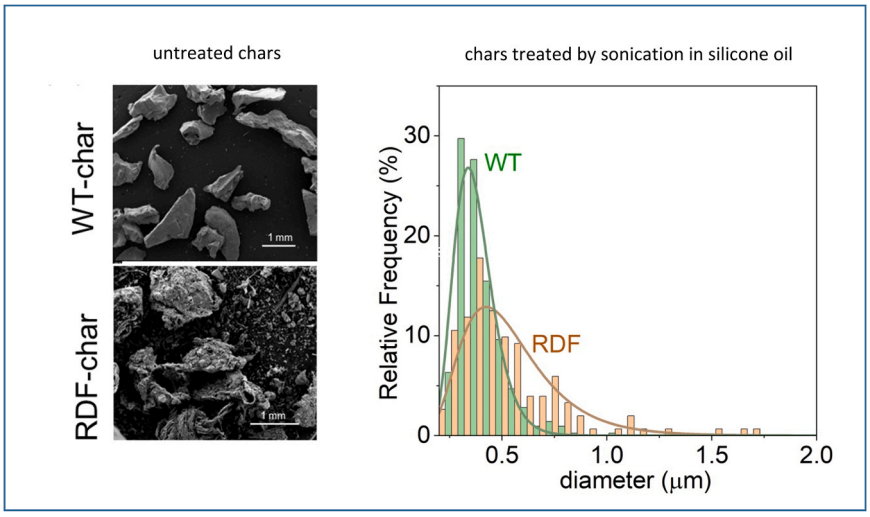

Fig. 3. left panel: representative SEM images of "as is" WT- and RDF- char samples. Right panel: size distribution functions of particles in WT- and RDF- char samples treated by sonication in silicone oil; in this plot continuous curves are the best lognormal distributions describing experimental data.

distribution of RDF-char is therefore shifted to slightly higher sizes with respect that of WT-char. It is also broader, with presence of rare big aggregates whose size extends to few μm, whereas the size distribution of WT-char particles looks sharper.

Despite the differences between the sizes found by XRD and SEM analysis, the general behavior is confirmed, being WT-char particles generally smaller than RDF-char ones, thus confirming the hypothesis that WT-char has the natural chemical tendency to form smaller domains, an aspect reflecting at different length-scales, from the nm-scaled crystalline or atomically ordered domains (see XRD) up to the μm-scaled polycrystalline particles and even to their mm-scaled assemblies (see SEM).

The differences in physico-chemical and morphological characteristics we have found will be essential to justify the difference in rheological performances we will show in the next section.

3.3. Bitumen characterization

3.3.1. Mechanical properties: G'@ 50 °C and T *

Through temperature-sweep measurements the evolution of both G' and G'' is monitored during a temperature ramp at a constant heating rate of 1 °C/min and at a frequency of 1 Hz. Fig. 4 A shows the time cure test for the pristine bitumen taken as a representative sample. From the figure, it can be seen that G' < G'' holds over the whole considered range. This behavior is shared by all the investigated samples and highlights that they all have a pseudoplastic fluid behavior. Both G′ and G′' are monotonously decreasing with temperature, showing that all samples are at higher values than their glass transition temperature, usually located slightly below 0 °C [48] at which G'' should have a maximum.

From the plot shown in Fig. 4 A the value of G′ at 50 °C (G′@50 °C) can be immediately derived. G'@ 50 °C is representative of the mechanical property of the material under usage condition (50 °C) and has been used in recent literature [49] as proper indicator of the bitumen rigidity.

As the temperature is increased, all the studied samples become progressively softer with G′ decreasing faster than G''. For temperature high enough, G′ suddenly drops, marking a real gel-to-sol transition. The temperature at which this transition takes place is labelled as T * (see Fig. 4 A for the graphical derivation). For temperatures higher than T * , the bitumen can be considered almost as a Newtonian fluid. From the microscopic point of view, in this situation the molecular thermal agitation, and consequently the molecular relaxation rate, is now sufficiently high to let the system accommodate for the mechanical distortion/perturbation. This gives purely flowing behavior and causes any elastic storage of mechanical energy to vanish.

G′@ 50 °C and T * values are shown in Fig. 4B for the various samples in a correlation plot. For ease of comparison, the values for aged bitumens are represented by darker dots.

Some comments are in order:

1) Effect of char addition:
   - The addition of char causes an increase in both G′@ 50 °C and T * . This effect is the consequence of the reinforcement of the bituminous structure at the macro-molecular level, given by the presence of fine particles. Addition of WT-char or RDF-char gives similar changes, with a slightly higher effect in the case of WT-char reasonably due to the higher carbon content allowing for a better distribution among the sample and/or more effective interactions with the organic-based structure of the bitumen.
   - Bitumen-char interactions can also be further highlighted by comparison with bitumens doped with $CaCO_3$, a standard inert filler used in most of the literature on bitumen and asphalt concretes. In fact, even the addition to bitumen of inert calcium carbonate results into a robustness increase, with an increment in both T * and G′@ 50 °C as clearly shown in ref [50]. However, in that work it turned out that bitumen loaded with 3% w/w of $CaCO_3$ has shown a 4 °C increase in T * and 3-fold increase in G′@ 50 °C. Conversely, our char samples lead to an increase in T * of 10.1 and 10.6 °C (RDF-char and WT-char, respectively, see Fig. 5). The increase in T * showed by RDF-char is therefore: (i) lower than that showed by WT-char and (ii) closer to that shown by bare $CaCO_3$ than that showed by WT-char. This can be the consequence of the high content in $CaCO_3$ possessed by RDF-char which reduces the potential effect of carbonaceous fraction of the char. With the appropriate proportions for the different concentration, in the presence of RDF-char and WT-char the change in T * is 25% and 33% respectively higher than in the presence of bare $CaCO_3$. No significant difference with the increase in G′@ 50 °C in the presence of $CaCO_3$ is instead observed.
2) Effect of aging:
   - Pristine and char-containing bitumens were subjected to artificial aging (see experimental section for details). Each aged bitumen shows higher values of G′@ 50 °C and T * then the corresponding unaged sample. This is expected, since the aging process always causes an increase of polar functional groups of the molecules in bitumens [51] with their ultimate aggregation and constrained dynamics;
   - Interestingly, the increase of both G′@ 50 °C and T * upon aging of bitumen containing WT-char is much more limited than that occurring in bitumen containing RDF-char. This is better shown in Fig. 5. Aging of reference bitumen causes an increase of T * of

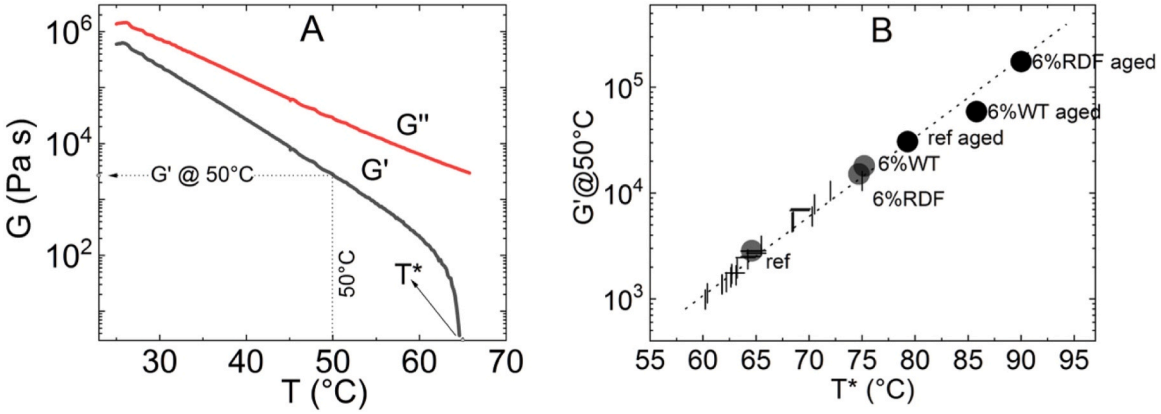

Fig. 4. (A) Plot of G′ and G'' as a function of temperature for a representative sample (pristine bitumen). The graphical derivation of G′@ 50 °C and T * is shown by the pointing arrows. (B) correlation between G′@ 50 °C and T * for the bituminous samples discussed in the present paper (circles), and comparison with data from literature (vertical and horizontal bars). For easier comparison, the values for aged bitumens are represented by darker points.

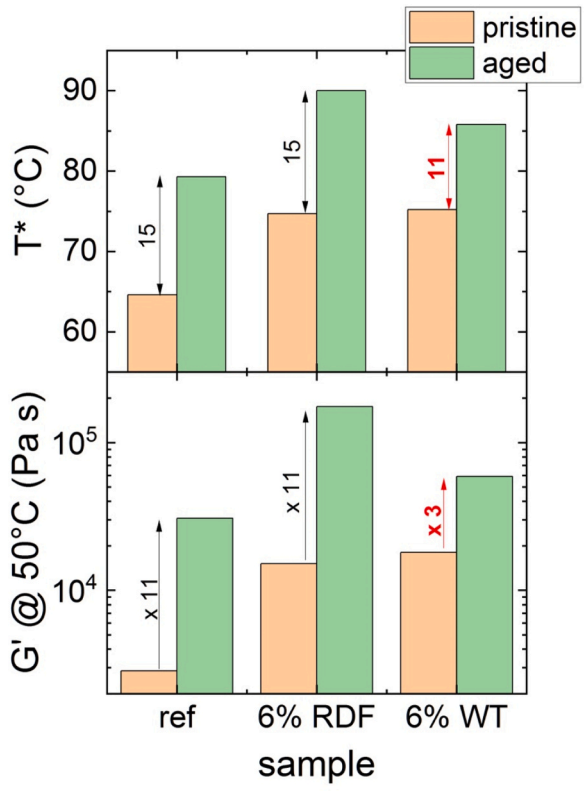

Fig. 5. T * and G′@ 50 °C values for all the samples, organized to show the effects of aging. Arrows indicate the increase in T * (upper panel) and the increase in G′@ 50 °C (lower panel).

about 15 °C. If the bitumen is reinforced with RDF-char, aging causes the same increase in T * : 15 °C. Instead, if bitumen is reinforced with WT-char, then the same aging causes an increase in T * of only 11 °C. This is a very important clue, since it unveils a certain anti-aging effect of WT-char. The same conclusion can be made by looking at the increase in G′@ 50 °C upon aging. Aging of reference bitumen causes a 11-fold increase in G′@ 50 °C. Same increment is observed for bitumen reinforced with the RDF-char. Instead, if the bitumen is reinforced with WT-char, then the same aging causes an increase in G′@ 50 °C of only three times.

- The observed effect could be ascribed to the more efficient interactions between the bituminous material and the surface of the WT-char particles thanks to their more carbonaceous nature giving more chemical compatibility. The stronger bitumen-char binding could better hinder some of the degrees of freedom in the molecules making part of the bituminous structure and consequently slow down the dynamic processes (translational, rotational, collective…) occurring in aging. All this ultimately gives an anti-aging effect. It could be argued that further chemical effects may derive from the presence of ZnS in WT-char: the presence of transition metals can give origin to further interactions between the metal atoms and the polar asphaltenes and/or the amphiphilic resins, as supposed in previous work [52], thus reinforcing the char-bitumen interactions.

The use of the correlation plot in Fig. 4B permits to easily notice that the G′@ 50 °C and T * are generally nicely correlated. Although they are two independent parameters (G′@50 °C refers to the Y-value of the G' plot in Fig. 4 A whereas T * refers to the X-value at which the curve drops in the same plot) they can be both considered as indicators of the reinforcing effect induced by the char and/or by the increase in rigidity induced by aging. The data in Fig. 4B are combined with literature data referring to bitumens reinforced with organic molecules [53] (polysaccharides, vertical bars) and inorganic fine particles [52] (horizontal bars) for comparison's sake. As it can be seen, all the sets of data are in accordance, suggesting quite a universal behavior.

Of course, different additives have different chemical characteristics and therefore they can give to different effects. In the case of char as filler, the increase in G′@ 50 °C and T * is quite high. This may be the consequence that char fine particles have simultaneously both the organic character and the fibrous structure of the polysaccharides, and the particle morphology of fine particles, thus giving enhanced effects.

Form rheological data the rutting parameter defined as G* /sin δ can be derived. The rutting parameter at 50 °C represents the mechanical property specifically under usage conditions [50]. It was found that the values meet the limits imposed by the Superior Performing Asphalt Pavements method under the Strategic Highway Research Program (Superpave SHRP) [54] being always higher than 1kPa for unaged samples.

3.3.2. *Arrhenius analysis: Ea and ln As*

The temperature dependence of both G′ and G'' allows further analysis. They both contribute to the viscosity (η), i.e. the ratio of G to angular frequency ω: [55].

$$\eta = \frac{G}{\omega}\frac{\sqrt{G'^2 + G''^2}}{\omega} \quad (1)$$

yielding information on the *total* amount of energy that the system absorbs. In other words, it represents the resistance to flow under oscillatory shear conditions.

The temperature dependence of η is reported in Fig. 6 A as ln η vs 1000/T (Arrhenius plot) for some representative samples. A linear trend of the data is observed, confirming the validity of the two wells potential model adopted by the Arrhenius approach.

The Arrhenius model to present the temperature dependence of viscosity has been chosen *not* according to custom but, rather, according to some considerations suggesting that the choice the Arrhenius model is the most adequate for this kind of samples in these conditions [56,57]. In addition, this choice offers the advantage of deriving parameters (Ea and ln As) with an intuitive physical meaning. In fact, though the application of the transition-state-theory [58] (TST) by Eyring of Arrhenius chemical kinetics to transport phenomena [59], data can be fitted by the Eq. 2:

$$\ln \eta * (T) = \ln As + \frac{Ea}{R}\cdot\frac{1}{T} \quad (2)$$

where *Ea* represents the activation energy to overcome for flowing to occur, R is the gas constant (8.314 J K^{-1} mol^{-1}) and *As* is the pre-exponential factor (frequency factor).

The derived *Ea* and ln *As* values are reported in Fig. 6B as correlation plot. *Ea* values are in the range 110–140 kJ mol^{-1} and are consistent with the values observed for other additivated bitumens [48]. The changes in *Ea*, after addition of char to the pristine bitumen, appear to be rather small suggesting that the essential dynamics is not perturbed much by the insertion of the char. This confirms, somehow, the char compatibility with the organic-based nature of bitumen. The only exception is represented by the bitumen reinforced with 6% WT-char after the aging process (6% WT aged): this sample shows a lower activation energy thus highlighting a decrease in the energetic barrier to overcome for flowing to occur. This effect does not take place in the corresponding unaged bitumen reinforced with 6% WT-char, so it cannot be ascribed only to the bare presence of the char but, rather, to the composition of effects due to the presence of that specific char and aging.

The lowering in Ea for this sample, from the microscopic point of view, could be ascribed, according to a model recently proposed in the literature [53], to a *shrinking* of the bituminous structure at the intermolecular level, most probably due to the high affinity with the

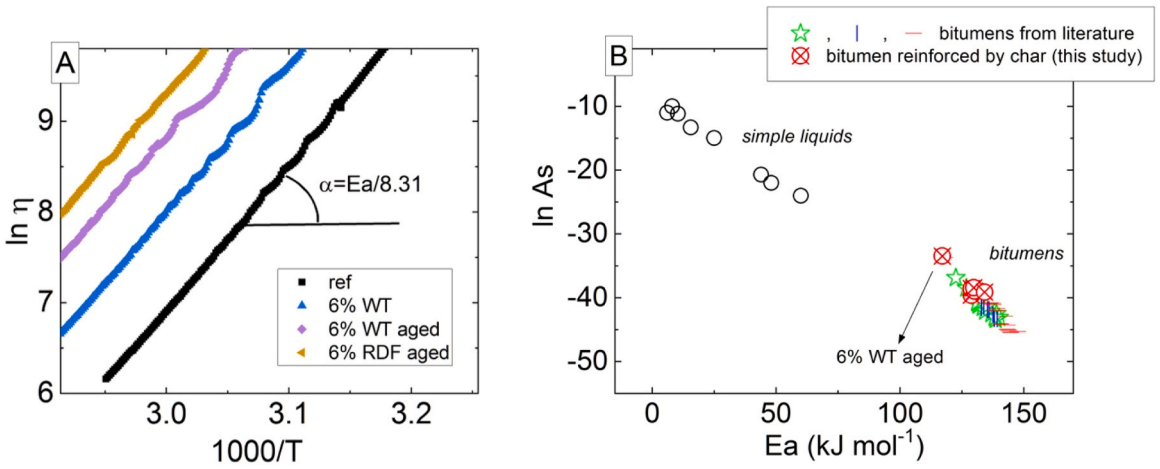

Fig. 6. (A) Arrhenius plot for some representative samples. The derivation of Ea is shown. (B) Correlation between the pre-exponential factor (ln *As*) and the activation energy (Ea). Data from the samples investigated in this work are represented as red crossed circles. Data from simple liquids (open circles) and from bitumens reinforced with polysaccharides (green stars), cellulose (vertical bars), mineral wastes (horizontal bars) are reported for comparison.

carbon-rich composition of the WT-char. This would consequently shrink the landscape of the two potential wells, which are brought closer giving a more pronounced overlap of the two potential curves and ultimately a lowering of the activation energy. It must be pointed out, however, that this model still needs further data and experiments to be reinforced, so this interpretation must be seen as just a reasonable hypothesis.

As for the pre-exponential factor (frequency factor), it represents the fraction of effective molecular collisions which are able to turn into the flowing process. In the fluidic structure of bitumen, in fact, flowing requires the formation and dislocation of molecular vacancies as concisely described by Byran et al. [60]: "*For any one molecule to move, other surrounding molecules must first give way and move into vacant lattice sites or "holes" to create a space for the molecule to enter*".

The low values of ln *As* would indicate a low number of effective molecular collisions which are able to turn into the flowing process, in agreement with the complex structure of the bitumen, the presence of high molecular mass molecules and the low viscosity. ln *As* turns out to be scarcely affected by the change in the additive used, despite the inherent variability associated to the ln As measurement [61–63]. This is in accordance with the small variations in *Ea* and confirms that the basic flowing process is maintained independently from the specific char used in this paper.

Interestingly, the pre-exponential factors are correlated with the activation energies (see Fig. 6B).

This behavior has been found in bitumens reinforced with organic additives (polysaccharides [53], cellulose [57]) and inorganic filler [52], whose data are reported, for comparison, in the same Fig. 6B. The accordance among all the sets of data is evident. Although there is not theory explaining such correlation yet, the data of this paper corroborate the pioneering observations in recent papers confirming that this correlation holds. From the applicative point of view, this correlation can be quite useful, since the temperature dependence of the viscosity for these systems can be predicted if only *one* Arrhenius parameter is known, since the other one is correlated to it.

Interestingly, the accordance holds also with simple liquids [64] (see Fig. 6B) despite the big differences in the values of viscosity, activation energies, pre-exponential factor and structure (bitumens are highly complex materials – see introduction - contrasting the structure of simple liquids). This suggests a quite universal behavior opening the door for a more general view of fluids. For this reason, we hope that the present data can be precious for further theoretical investigation in order to model such a universal behavior.

4. Conclusions

This study showed how products from the pyrolysis of wastes can be used to improve bitumens. The addition of char from the pyrolysis of tires (WT) or of Refuse Derived Fuels (RDF) to a typical 50/70 bitumen gave increased shear modulus and higher resistance to temperature, as revealed by the increased gel-to-sol transition temperature. The effect was found to be higher than standard inert filler. Interestingly, the char from pyrolysis of WT showed to possess also anti-aging effect, contrasting the increase in rigidity generally occurring during aging. These effects, with the support of the Arrhenius analysis of rheological data, were justified by the high carbon content of the char, in particular that of WT-char, giving char chemical compatibility with the organic nature of the bitumen and reasonably allowing for its homogeneous inclusion within the bituminous molecular matrix through effective interactions. The presented data can give a framework of utmost importance for future efficient production of char and its application, with an eye to environmental protection.

Funding

This research was funded by @CNR Project ReScA "Recupero degli scarti da pirolisi di rifiuti urbani per potenziare e ripristinare asfalti", decision of Administration Council dated 21 dicembre 2021.

CRediT authorship contribution statement

Valentina Gargiulo: Formal analysis, Data curation, Validation, Writing-original draft, Writing - review and editing. **Michela Alfe** Conceptualization, Data curation, Funding acquisition, Project administration, Supervision, Validation, Writing-original draft, Writing - review and editing. **Giovanna Ruoppolo:** Data curation, Supervision, Validation, Writing - review and editing. **Francesco Cammarota:** Formal analysis, Data curation, Validation. **Cesare Oliviero Rossi** Supervision, Resources, conceptualization. **Valeria Loise** Investigation, Data curation, Visualization. **Michele Porto** Investigation, Data curation, Visualization. **Pietro Calandra** Methodology, Investigation, Conceptualization, Writing - original draft, Writing - review & editing, funding acquisition. **Mikolaj Pochylski** Investigation, Visualization. **Jacek Gapinski** Investigation, Data curation. **Paolino Caputo** Investigation, Data curation, Visualization.

Declaration of Competing Interest

The authors declare that they have no known competing financial interests or personal relationships that could have appeared to influence the work reported in this paper.

Data Availability

Data will be made available on request.

Acknowledgments

The assistance of Luciano Cortese (STEMS-CNR) for SEM-EDX analysis and Fernando Stanzione (STEMS-CNR) for ICP-MS analysis was kindly acknowledged. M. Alfé and V. Gargiulo also acknowledge the contribution of the WIRE Cost Action CA20127.

Appendix A. Supporting information

Supplementary data associated with this article can be found in the online version at doi:10.1016/j.colsurfa.2023.132199.

References

[1] M. Geissdoerfer, P. PSavaget, N.M.P. Bocken, E. Hultink, The circular economy – a new sustainability paradigm? J. Clean. Prod. 143 (2017) 757–768, https://doi.org/10.1016/j.jclepro.2016.12.048.
[2] Manifesto for a Resource Efficient Europe. ⟨https://ec.europa.eu/commission/presscorner/detail/en/MEMO_12_989,⟩ 2013 (accessed February 2023).
[3] J. Lehmann, S. Joseph, Biochar for Environmental Management: Science. Technology and Implementation, 2nd ed..,, Routledge,, London, 2015.
[4] G. Sollazzo, S. Longo, M. Cellura, C. Celauro, Impact analysis using life cycle assessment of asphalt production from primary data, Sustainability 12 (24) (2020) 10171, https://doi.org/10.3390/su122410171.
[5] P. Caputo, A.A. Abe, V. Loise, M. Porto, P. Calandra, R. Angelico, C. Oliviero Rossi, The role of additives in warm mix asphalt technology: an insight into their mechanisms of improving an emerging technology, Nanomater 10 (2020) 1202, https://doi.org/10.3390/nano10061202.
[6] P. Caputo, P. Calandra, V. Loise, A. Le Pera, A.-M. Putz, A.A. Abe, L. Madeo, B. Teltayev, M.L. Luprano, M. Alfè, V. Gargiulo, G. Ruoppolo, C. Oliviero Rossi, When physical chemistry meets circular economy to solve environmental issues: how the ReScA project aims at using waste pyrolysis products to improve and rejuvenate bitumens, Sustainability 14 (2022) 5790, https://doi.org/10.3390/su14105790.
[7] E.A. Taborda, C. Franco, M.A. Ruiz, V. Alvarado, F.B. Cortés, Experimental and theoretical study of viscosity reduction in heavy crude oils by addition of nanoparticles, Energ. Fuels 31 (2017) 1329–1338, https://doi.org/10.1021/acs.energyfuels.6b02686.
[8] H. Wang, I.L. Al-Qadi, A.F. Faheem, H.U. Bahia, S.H. Yang, G.H. Reinke, Effect of mineral filler characteristics on asphalt mastic and mixture rutting potential, Transp. Res. Rec. 5 (2011) 33–39, https://doi.org/10.3141/2208-2205.
[9] J.M. Krishnan, C.L. Rao, Mechanics of air voids reduction of asphalt concrete using mixture theory, Int. J. Eng. Sci. 38 (2000) 1331–1354, https://doi.org/10.1016/S0020-7225(99)00075-0.
[10] A. Rahman, S.A. Ali, S.K. Adhikary, Q.S. Hossain, Effect of fillers on bituminous paving mixes: an experimental study, J. Eng. Sci. 3 (2012) 121–127, https://doi.org/10.17577/IJERTV8IS050070.
[11] A. Zhambolova, A.L. Vocaturo, Y. Tileuberdi, Y. Ongarbayev, P. Caputo, I. Aiello, C.O. Rossi, N. Godbert, Functionalization and modification of bitumen by silica nanoparticles, Appl. Sci. 10 (17) (2020) 6065, https://doi.org/10.3390/app10176065.
[12] P. Caputo, M. Porto, R. Angelico, V. Loise, P. Calandra, C. Oliviero Rossi, Bitumen and asphalt concrete modified by nanometer-sized particles: Basic concepts, the state of the art and future perspectives of the nanoscale approach, Adv. Colloid Interface Sci. 285 (2020), 102283, https://doi.org/10.1016/j.cis.2020.102283.
[13] A.T. Sipra, N. Gao, H. Sarwar, Municipal solid waste (MSW) pyrolysis for bio-fuel production A review ofeffects of MSW components and catalysts, Fuel Process. Technol. 175 (2018) 131–147, https://doi.org/10.1016/j.fuproc.2018.02.012.
[14] J. Aguado, D.P. Serrano, S.M. Guillermo, S. Madrid, Feedstock recycling of polyethylene in a two-step thermo-catalytic reaction system, J. Anal. Appl. Pyrolysis 79 (1) (2007) 415–423, https://doi.org/10.1016/j.jaap.2006.11.008.
[15] H.M. Kadlimatti, B. Raj Mohan, M.B. Saidutta, Bio-oil from microwave assisted pyrolysis of food waste-optimization using response surface methodology, Biomass- Bioenergy 123 (2019) 25–33, https://doi.org/10.1016/j.biombioe.2019.01.014.
[16] I. Romeo, F. Olivito, A. Tursi, V. Algieri, A. Beneduci, G. Chidichimo, L. Maiuolo, E. Sicilia, A. De Nino, Totally green cellulose conversion into bio-oil and cellulose citrate using molten citric acid in an open system: synthesis, characterization and computational investigation of reaction mechanisms,RSC, Adv 10 (2020) 34738–34751, https://doi.org/10.1039/D0RA06542K.
[17] L. Maiuolo, F. Olivito, V. Algieri, P. Costanzo, A. Jiritano, M.A. Tallarida, A. Tursi, C. Sposato, A. Feo, A. De Nino, Synthesis, characterization and mechanical properties of novel bio-based polyurethane foams using cellulose-derived polyol for chain extension and cellulose citrate as a thickener additive, Polymers 13 (2021) 2802, https://doi.org/10.3390/ polym13162802.
[18] P. McKendry, Energy production from biomass (Part 1): overview of biomass, Bioresour. Technol. 83 (1) (2002) 37–46, https://doi.org/10.1016/s0960-8524(01)00118-3.
[19] A.K. Hossain, P. Davies, A Pyrolysis liquids and gases as alternative fuels in internal combustion engines – a review, Renew. Sust. Energ. Rev. 21 (2010) 165–189, https://doi.org/10.1016/j.rser.2012.12.031.
[20] F. Abnisa, W.M.A.W. Daud, A review on co-pyrolysis of biomass: an optional technique to obtain a high-grade pyrolysis oil, Energy Convers. Manag. 87 (2014) 71–85, https://doi.org/10.1016/j.enconman.2014.07.007.
[21] M.S. Reza, C.S. Yun, S. Afroze, N. Radenahmad, M.S.A. Bakar, R. Saidur, J. Taweekun, A.K. Azad, Preparation of activated carbon from biomass and its' applications in water and gas purification, a review, Arab. J. Basic Appl. Sci. 27 (2020) 208–238, https://doi.org/10.1080/25765299.2020.1766799.
[22] S. Chandra, P. Jagdale, I. Medha, A.K. Tiwari, M. Bartoli, A. De Nino, F. Olivito, Biochar-supported TiO2-based nanocomposites for the photocatalytic degradation of sulfamethoxazole in water—a review, Toxics 9 (11) (2021) 313, https://doi.org/10.3390/toxics9110313. ⟨https://doi.org/10.3390/toxics9110313⟩.
[23] S. Zhao, B. Huang, X.P. Ye, X. Shu, X. Jia, Utilizing bio-char as a bio-modifier for asphalt cement: a sustainable application of bio-fuel by-product, Fuel 133 (2014) 52–62, https://doi.org/10.1016/j.fuel.2014.05.002.
[24] A. Rajib, S. Saadeh, P. Katawal, B. Mobasher, E.H. Fini, Enhancing biomass value chain by utilizing biochar as a free radical scavenger to delay ultraviolet aging of bituminous composites used in outdoor construction, Resour. Conserv. Recycl. 168 (2021), 105302, https://doi.org/10.1016/j.resconrec.2020.105302.
[25] A. Kumar, R. Choudhary, A. Kumar, Characterization of thermal storage stability of waste plastic pyrolytic char modified asphalt binders with sulfur, PLoS One 16 (2021), e0248465.
[26] F.R. Amin, Y. Huang, Y. He, R. Zhang, G. Liu, C. Chen, Biochar applications and modern techniques for characterization, Clean. Technol. Environ. Policy 18 (2016) 1457–1473, https://doi.org/10.1007/s10098-016-1218-8.
[27] M. Alfè, V. Gargiulo, M. Porto, R. Migliaccio, A. Le Pera, M. Sellaro, C. Pellegrino, A.A. Abe, M. Urciuolo, P. Caputo, P. Calandra, V. Loise, C.Oliviero Rossi, G. Ruoppolo, Pyrolysis and gasification of a real refuse-derived fuel (RDF): the potential use of the products under a circular economy vision, Molecules 27 (2022) 8114, https://doi.org/10.3390/molecules27238114.
[28] N. Gao, F. Wang, C. Quan, L. Santamaria, G. Lopez, P.T. Williams, Tire pyrolysis char: Processes, properties, upgrading and applications, Prog. Energy Combust. Sci. 93 (2022), 101022, https://doi.org/10.1016/j.pecs.2022.101022.
[29] D. Petrauskas, S. Ullah, Manufacture and storage of bitumens, in: R.N. Hunter, A. Self, J. Read (Eds.), The Shell bitumen handbook, ICE Publishing, London, 2003, p. 29.
[30] V. Loise, P. Calandra, A.A. Abe, M. Porto, C. Oliviero Rossi, M. Davoli, P. Caputo, Additives on aged bitumens: what probe to distinguish between rejuvenating and fluxing effects? J. Mol. Liq. 339 (2021), 116742 https://doi.org/10.1016/j.molliq.2021.116742.
[31] P. Caputo, G. Ventruti, P. Calandra, M. Porto, B. Teltayev, R. Angelico, C. Oliviero Rossi, Searching effective indicators of microstructural changes in bitumens during aging: A multi-technique approach, Colloids Surf. A: Physicochem. Eng. 64120 (2022), 128529, https://doi.org/10.1016/j.colsurfa.2022.128529.
[32] E. Shaffie, A.K. Arshad, A. Alisibramulisi, J. Ahmad, W. Hashim, Z.A. Rahman, R. Jaya, Effect of mixing variables on physical properties of modified bitumen using natural rubber latex, Int. J. Civ. Eng. Technol. 9 (2018) 1812–1821.
[33] C. Oliviero Rossi, S. Ashimova, P. Calandra, M.P. De Santo, R. Angelico, Mechanical resilience of modified bitumen at different cooling rates: a rheological and atomic force microscopy investigation, Appl. Sci. 7 (2017) 779, https://doi.org/10.3390/app7080779.
[34] R. Hunter, A. Self, J. Read. The Shell Bitumen Handbook, 6th ed.,, ICE Publishing,, London, 2015.
[35] G. Lu, S. Zhang, S. Xu, N. Dong, H. Yu, Rheological behavior of warm mix asphalt modified with foaming process and surfactant additive, Crystals 11 (2021) 410, https://doi.org/10.3390/cryst11040410.
[36] E. Remišová, V. Zatkaliková, F. Schlosser, Study of rheological properties of bituminous binders in middle and high temperatures, Civ. Environ. Eng. 12 (12) (2018) 13–20, https://doi.org/10.1515/cee-2016-0002.
[37] H. Barnes, J.F. Hutton, K. Walters, An introduction to rheology, Elsevier Science Publishers,, Amsterdam, 1989.
[38] S.-Q. Li, Q. Yao, S.-E. Wen, Y. Chi, J.-H. Yan, Properties of pyrolytic chars and activated carbons derived from pilot-scale pyrolysis of used tires, J. Air Waste Manag. Assoc. 55 (9) (2005) 1315–1326, https://doi.org/10.1080/10473289.2005.10464728.
[39] C. Arnal, M. Alfè, V. Gargiulo, A. Ciajolo, M.U. Alzueta, A. Millera, R. Bilbao, Characterization of soot, in: F. Battin-Leclerc, J.M. Simmie, E. Blurock (Eds.), Developing Detailed Chemical Kinetic Models series: Green Energy and technology, Springer-Verlag, London, 2013, pp. 333–362.
[40] P. Napolitano, M. Alfè, C. Guido, V. Gargiulo, V. Fraioli, C. Beatrice, Particle emissions from a HD SI gas engine fueled with LPG and CNG, Fuel 269 (2020), 117439, https://doi.org/10.1016/j.fuel.2020.117439.
[41] K. Frikha, L. Limousy, J. Pons Claret, C. Vaulot, K.F. Pérez, B.C. Garcia, S. Bennici, Potential valorization of waste tires as activated carbon-based adsorbent for

organic contaminants removal, Materials 15 (2022) 1099, https://doi.org/10.3390/ma15031099.
[42] F.A. López, T.A. Centeno, O. Rodríguez, F.J. Alguacil, Preparation and characterization of activated carbon from the char produced in the thermolysis of granulated scrap tyres, J. Air Waste Manag. Assoc. 63 (5) (2013) 534–544, https://doi.org/10.1080/10962247.2013.763870.
[43] H. Darmstadt, C. Roy, S. Kaliagljine, Characterization of pyrolytic carbon blacks from commercial tire pyrolysis, Carbon 33 (1995) 1449–1455, https://doi.org/10.1016/0008-6223(95)00096-V.
[44] S. Seng-Eiad, S. Jitkarnka, Untreated and HNO_3-treated pyrolysis char as catalysts for pyrolysis of waste tire: In-depth analysis of tire-derived products and char characterization, J. Anal. Appl. Pyrolysis 122 (2016) 151–159, https://doi.org/10.1016/j.jaap.2016.10.004.
[45] H. Haykiri-Acma, G. Kurt, S. Yaman, Properties of biochars obtained from rdf by carbonization: influences of devolatilization severity, Waste Biomass-.-. Valor 8 (2017) 539–547, https://doi.org/10.1007/s12649-016-9610-5.
[46] M. Bhatt, S. Wagh, A. Gupta Chakinala, K. Kishore Pant, T. Sharma, J. Bhalchandra Joshi, K. Shah, A. Sharma, Conversion of refuse derived fuel from municipal solid waste into valuable chemicals using advanced thermo-chemical process, J. Clean. Prod. 329 (2021), 129653, https://doi.org/10.1016/j.jclepro.2021.129653.
[47] N. Lushinga, L. Cao, Z. Dong, Effect of silicone oil on dispersion and low-temperature fracture performance of crumb rubber asphalt, Adv. Mater. Sci. Eng. 2019 (2019) 8602562, https://doi.org/10.1155/2019/8602562.
[48] P. Calandra, P. Caputo, M.P. De Santo, L. Todaro, V. Turco Liveri, C. Oliviero Rossi, Effect of additives on the structural organization of asphaltene aggregates in bitumen, Constr. Build. Mater. 199 (2019) 288–297, https://doi.org/10.1016/j.conbuildmat.2018.11.277.
[49] C. Somé, A. Pavoine; E. Chailleux, L. Andrieux, L. DeMArco, S. Philippe Da, B. Stephan, Rheological behaviour of vegetable oil-modified asphaltite binders and mixes. In Proceedings of the 6th Eurasphalt & Eurobitume Congress, Prague, Czech, 1–3 June 2016; Paper No. EE.2016.222.
[50] C. Oliviero Rossi, P. Caputo, V. Loise, D. Miriello, B. Teltayev, R. Angelico, Role of a food grade additive in the high temperature performance of modified bitumens, Colloids Surf. A: Physicochem. Eng. 532 (2017) 618–624, https://doi.org/10.1016/j.colsurfa.2017.01.025.
[51] V. Loise, P. Caputo, M. Porto, P. Calandra, R. Angelico, C. Oliviero Rossi, A review on bitumen rejuvenation: mechanisms, materials, methods and perspectives, Appl. Sci. 9 (2019) 4316, https://doi.org/10.3390/app9204316.
[52] P. Calandra, S. Quaranta, B. Apolo Miranda Figueira, P. Caputo, M. Porto, C. Oliviero Rossi, Mining wastes to improve bitumen performances: an example of circular economy, J. Colloid Interface Sci. 614 (2022) 277–287, https://doi.org/10.1016/j.jcis.2022.01.106.
[53] M. Porto, P. Caputo, V. Loise, G. De Filpo, C. Oliviero Rossi, P. Calandra, Polysaccharides-reinforced bitumens: specificities and universality of rheological behavior, Appl. Sci. 9 (2019) 5564, https://doi.org/10.3390/app9245564.
[54] T.W. Kennedy, G. Huber, E.T. Harrigan, R.J. Cominsky, C.S. Hughes, H.L. Quintus, Von; J.S. Moulthrop, Superior Performing Asphalt Pavements (Superpave): The Product Of The Shrp Asphalt Research Program, National Research Council, 1994.
[55] C.W. Macosko, Rheology: Principles, Measurements, and Applications, Wiley Publishing,, USA, 1994.
[56] P. Caputo, P. Calandra, R. Vaiana, V. Gallelli, G. De Filpo, C. Oliviero Rossi, Preparation of asphalt concretes by gyratory compactor: a case of study with rheological and mechanical aspects, Appl. Sci. 10 (2020) 8567, https://doi.org/10.3390/app10238567.
[57] P. Caputo, V. Algieri, L. Maiuolo, A. De Nino, E. Sicilia, F. Ponte, P. Calandra, C. Oliviero Rossi, Waste additives as biopolymers for the modification of bitumen: mechanical performances and structural analysis characterization, Colloids Surf. A: Physicochem. Eng. 663 (2023) 131079, https://doi.org/10.1016/j.colsurfa.2023.131079.
[58] H. Eyring, The activated complex in chemical reactions, J. Chem. Phys. 3 (1935) 107–115, https://doi.org/10.1063/1.1749604.
[59] H.J.V. Tyrrell, K.R. Harris, Diffusion in Liquids, Butterworths,, London, UK, 1984.
[60] J. Byran, A. Kantzas, C. Bellehumer, Oil-viscosity predictions from low-field NMR measurements, 2005. SPE Res Eval. Eng. 8 (1) (2005) 44–52, https://doi.org/10.2118/89070-PA.
[61] A. Rabbani, D.R. Schmitt, Ultrasonic shear wave reflectometry applied to the determination of the shear moduli and viscosity of a viscoelastic bitumen, Fuel 232 (2018) 506–518, https://doi.org/10.1016/j.fuel.2018.05.175.
[62] Y. Zhao, H.G. Machel, Viscosity and other rheological properties of bitumen from the Upper Devonian Grosmont reservoir, Alberta, Canada, AAPG Bull. 96 (1) (2012) 133–153, https://doi.org/10.1306/04261110180.
[63] K.A. Miller, L.A. Nelson, R.M. Almond, Should you trust your heavy oil viscosity measurement? J. Can. Pet. Technol. 45 (04) (2006).
[64] A. Messaâdi, N. Dhouibi, H. Hamda, F.B.M. Belgacem, Y.H. Adbelkader, N. Ouerfelli, A.H. Hamzaoui, A new equation relating the viscosity arrhenius temperature and the activation energy for some newtonian classical solvents, J. Chem. 2015 (2015), 163262, https://doi.org/10.1155/2015/163262.